AIAA JOURNAL
Vol. 36, No. 8, August 1998

Technical Notes

TECHNICAL NOTES are short manuscripts describing new developments or important results of a preliminary nature. These Notes cannot exceed 6 manuscript pages and 3 figures; a page of text may be substituted for a figure and vice versa. After informal review by the editors, they may be published within a few months of the date of receipt. Style requirements are the same as for regular contributions (see inside back cover).

Use of Piezoelectric Actuators for Airfoil Separation Control

A. Seifert,* S. Eliahu,† D. Greenblatt,†
and I. Wygnanski‡
Tel-Aviv University, Tel-Aviv 69978, Israel

Introduction

THE addition of cyclic vortical perturbations to a boundary layer delays flow separation and eliminates its associated adverse effects in an effective manner.[1] The range of Reynolds numbers at which the experiments were carried out was recently extended to 38×10^6, demonstrating the validity of the control parameters at flight Reynolds numbers.[2] However, most of the experiments performed to date have used external laboratory devices to generate the perturbations, and the net efficiency of the system has not been considered. Presently, surface-mounted piezoelectric actuators are used to excite the turbulent boundary layer upstream of separation, where the actuators interact directly with the boundary layer. The actuators are rigid and do not attenuate with increased aerodynamic loading up to the maximum tested speed of 30 m/s. It is demonstrated that these actuators are effective as well as energy efficient.

Brief Description of Experiment

The actuators were of the Unimorph type, where each piezoceramic plate is bonded to a metal plate, 35 mm long and 60 mm wide. The resonance frequency of each actuator was approximately 170 Hz and, when driven by a sine wave in still air, its tip vibrated to a maximum of 13 mm peak-to-peak (ptp). An Israel Aircraft Industries (IAI) Pr8-40-SE airfoil was used, with a chord c of 360 mm and a span of 609 mm (the test-section width). A transition strip (grit no. 100) was located at the leading-edge region of the airfoil (from $X/c = 0.03$ on the lower surface to $X/c = 0.05$ on the upper surface). The experiment was conducted in a closed-loop, low-turbulence, low-speed ($\leq$40 m/s) wind tunnel with a 2-ft-wide $\times$ 3-ft-high $\times$ 20-ft-long test section. Twenty-seven differential pressures were measured along the centerline of the airfoil surface (for lift, moment, and form drag) and in its wake (for total drag) using a wake rake located four chordlengths downstream of the airfoil midchord. The pressure transducers were accurate within $\pm 1\%$ (of the $\pm$100-mm H_2O full scale). Because of the exploratory nature of the experiment, only time-averaged pressures were measured. The effect of the surface pressure fluctuations on lift and pitching moment was negligible because of the long sampling time (5 s). The wake unsteadiness is expected to be very low at the wake-rake position and to be averaged out by the long sampling duration. The power provided to the actuators was calculated from measured ac voltage, current, and phase lag. The uncertainty was ± 0.02 in C_l, ± 0.0010 in C_d, $\pm 2\%$ in U_∞ and ± 5 in the maximum airfoil power efficiency $\eta_{\max}$. The data were not corrected for tunnel-wall interference because the expected corrections[3] (-3% in $C_{l_{\max}}$, -5% in the corresponding C_d, and $+2\%$ in the corresponding L/D) are of the same magnitude as the experimental uncertainty. Furthermore, the major consideration in this Note was the relative change from baseline to controlled flow, which is only marginally affected by interference, whereas the corrections are not strictly valid near stall.

Installation of Actuators

A channel 35.5 mm wide, 605 mm long, and 8.5 mm deep was machined in the airfoil upper surface, starting at $X/c = 41\%$ (see insert in Fig. 1). Ten actuators were mounted along the span of the airfoil, flush-mounted to its upper surface, with 0.5-mm gaps between adjacent actuators and between the actuators and the cavity walls. Each actuator was isolated electrically from the airfoil and connected individually to the driving system to allow full control of the phase and amplitude. The resonance frequency of the actuators was tuned identically to within ± 0.5 Hz.

Two modes of excitation were tested: a two-dimensional mode, where all actuators operated at identical amplitude and phase, and a three-dimensional mode, where the amplitudes were identical but the phase of alternate actuators was reversed (as shown schematically in Fig. 1). Two important differences between these modes were noted. First, when the actuators were operated in identical phase, a two-dimensional disturbance was generated, whereas the three-dimensional mode generated a complicated pattern of alternating streamwise vortices (introduced by the vertical shear layers between the actuators) and a staggered two-dimensional wave (introduced by the common frequency and amplitude). Second, when the actuators operate in the two-dimensional mode they compress the cavity air when moving downward, whereas in the three-dimensional mode, the downward motion of alternating actuators assists the upward motion of their immediate neighbors. This phenomenon results in a factor of about four between the power required to generate approximately the same mechanical amplitude from the two modes of motion (2.4 vs 0.65 W per actuator for 6-mm ptp mechanical amplitude for the two-dimensional and

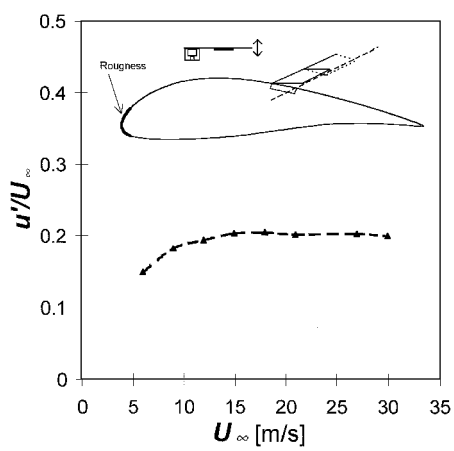

Fig. 1 Excited boundary-layer velocity perturbation vs freestream velocity (α = 8 deg, f = 170 Hz, 3.5 mm downstream from the actuator, Y = 1 mm, mechanical amplitude $\approx$ 3 mm, two-dimensional mode). The insert shows the IAI Pr8 airfoil, the cavity, and a schematic description of the actuator alone and as it operates in the three-dimensional mode.

Received Jan. 26, 1998; revision received May 6, 1998; accepted for publication May 6, 1998.

*Department Engineer, Department of Fluid Mechanics and Heat Transfer; currently NRC Researcher, MS 170, NASA Langley Research Center, Hampton, VA 23681. Member AIAA.

†Graduate Student, Department of Fluid Mechanics and Heat Transfer.

‡Professor, Department of Fluid Mechanics and Heat Transfer. Fellow AIAA.

Table 1 Summary of airfoil performance enhancement due to active separation control

Parameter	Explanation	Mode		
		Baseline	Two dimensional	Three dimensional
$C_{l_{\max}}$	Maximum lift coefficient	1.26	1.51	1.54
α of $C_{l_{\max}}$	Incidence at $C_{l,\max}$	8	10	12
$C_{d,\min}$	Minimum drag coefficient	0.0186	0.0145	0.0155
C_l of $C_{d,\min}$		0.49	0.71	0.71
$L/D_{,\max}$	Maximum lift/drag ratio	43	62	56.5
C_l of $L/D_{,\max}$		0.9	1.3	1.1
L/D at $C_{l_{\max}}/1.21$		43	61	53
$\eta_{\max}$	Maximum power efficiency	43	38	48
C_l at $\eta_{\max}$		0.89	1.40	1.09
$C_d + C_E$ at $\eta_{\max}$	Total power coefficient	0.0206	0.0374	0.0228

three-dimensional modes, respectively). Three-dimensional effects caused by the three-dimensional mode of excitation were not investigated. However, examination of spanwise pressure nonuniformity[4] indicates that it persists about one device width downstream of the actuator with no upstream three-dimensional effects. Because most of the lift increment is generated upstream of the device, we expect the pressure nonuniformity downstream of the device on the lift to be in the specified uncertainty level. The three-dimensional nature of the near wake is eliminated downstream at the specified wake measurement station.

Actuator Performance

Three basic selection criteria for a suitable separation control actuator are appropriate frequency, sufficient amplitude, and rigidity to withstand aerodynamic and structural loading. With a resonance frequency of 170 Hz, a midchord mounting, and a freestream velocity of $U_\infty = 23.5$ m/s, the actuators provide a reduced frequency, $F^+ = f(c/2)/U_\infty = 1.2$, which is effective for separation control.[1] The mechanical amplitude of a separation control actuator that relies on direct interaction with the boundary layer to generate the vorticity fluctuations should be comparable to the thickness of the shear layer, which is its source of steady vorticity. The installed actuators were capable of more than 6-mm ptp vibration, which was of the same order as the turbulent boundary-layer thickness at high α. To test for rigidity, an actuator was mounted on the airfoil together with a calibrated hot wire that was located 3.5 mm downstream of it and about 1 mm above the surface. The airfoil was positioned at $\alpha = 8$ deg, and U_∞ was altered while the actuator was operating at resonance. Figure 1 presents the measured boundary-layer velocity perturbation. It became evident that this actuator was capable of generating fluctuations at a level corresponding to $0.2U_\infty$ at $U_\infty \leq 30$ m/s. The maximum u'/U_∞ was about 0.25 at somewhat larger Y. Larger u'/U_∞ were not expected because the actuator acts as a mixer across the boundary layer, where the potential is a velocity fluctuation ranging from zero to U_∞ or $u'/U_\infty \approx 0.33$. The maximum velocity of the actuator tip is estimated as $\omega A = 2\pi f A \approx 3.2$ m/s or $0.136U_\infty$.

Airfoil Performance

The improvement in the airfoil performance was measured at a single Reynolds number $R_c = 0.55 \times 10^6$, using a tripped boundary layer and comparing the two modes of excitation—two dimensional and three dimensional—to the baseline.

The lift, drag, L/D, and figure of merit (FM, defined later) of the separation-controlled airfoil are presented in Figs. 2, 3, 4, and 5, respectively. Table 1 contains a summary of important parameters and relevant values.

The input power coefficient is defined by

$$C_E = \frac{W_i}{\frac{1}{2}\rho S U_\infty^3}$$

and the airfoil power efficiency η is then

$$\eta = \frac{C_l}{C_d + C_E}$$

where S is the airfoil planview area and W_i is the power applied to the 10 actuators across the airfoil span. The power coefficients were

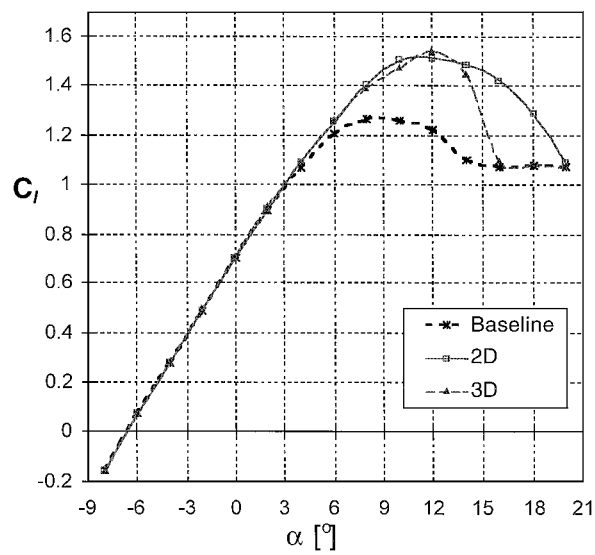

Fig. 2 Lift vs angle of attack (tripped boundary layer, $R_c = 0.55 \times 10^6$, $F^+ = 1.2$).

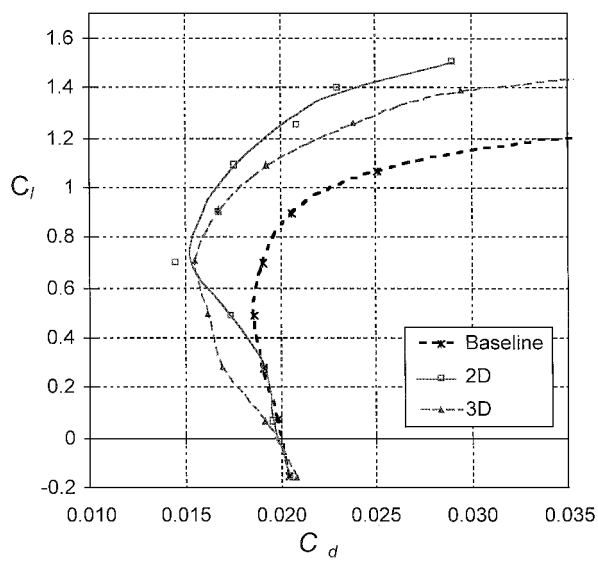

Fig. 3 Lift vs drag (tripped boundary layer, $R_c = 0.55 \times 10^6$, $F^+ = 1.2$).

0.0143 and 0.0035 for the two-dimensional and three-dimensional modes, respectively. To assess the benefits possibly obtained by operating the separation-control actuators, we define an FM as the ratio between the power and the aerodynamic efficiencies:

$$\text{FM} = \frac{\eta}{C_l/C_d}$$

This quantity can be used as a criterion for operating the separation-control device and also to determine which mode to use at a specific flight condition.

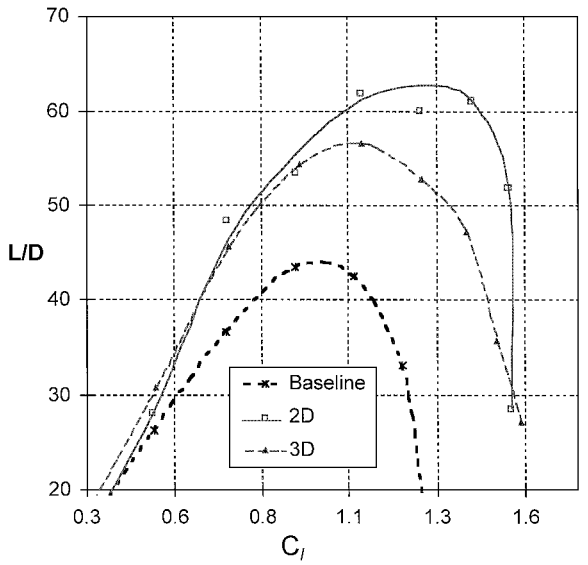

Fig. 4 Lift/drag ratio vs lift (tripped boundary layer, $R_c = 0.55 \times 10^6$, $F^+ = 1.2$).

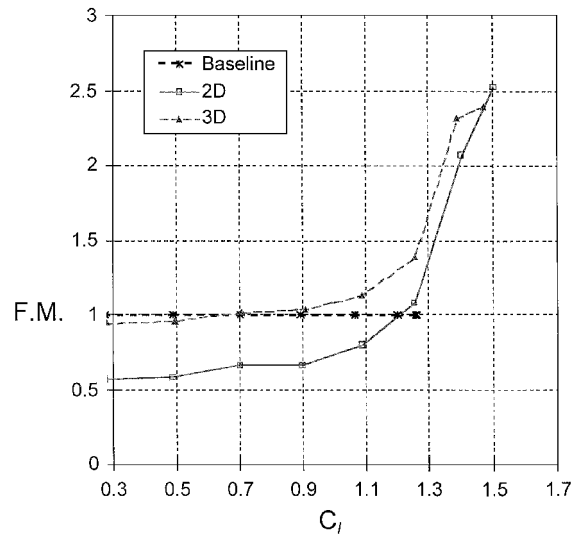

Fig. 5 FM vs lift (tripped boundary layer, $R_c = 0.55 \times 10^6$, $F^+ = 1.2$).

Observing the various aspects of the airfoil performance, one can identify the following trends.

1) $C_{l_{max}}$ increases by 20–22%, regardless of the excitation mode, because of the delay of stall by 2–4 deg. Considering the lower power consumption of the three-dimensional mode, it is certainly preferred for lift enhancement at landing configuration.

2) The two-dimensional mode generates a milder poststall behavior than the three-dimensional mode; therefore it is expected to perform better in hysteresis prevention and dynamic stall suppression.

3) The baseline drag diverges rapidly for $C_l > 0.7$; the drag divergence of the two-dimensional and three-dimensional excited modes is milder. At $C_l \geq 1.1$ the drag of the two-dimensional mode is the smallest.

4) The two-dimensional mode generates the highest L/D at the highest C_l. The combination of high C_l at the highest L/D and mild poststall behavior makes the two-dimensional mode a suitable candidate for takeoff configuration.

5) When power efficiency is considered, in conjunction with the FM (Fig. 5), it becomes evident that it is expedient to operate in the three-dimensional mode at $C_l > 0.7$ and in the two-dimensional mode at $C_l > 1.2$.

The physical mechanism describing the nature of spanwise and streamwise vorticity generation by the two-dimensional and three-dimensional modes and the interaction between the separating boundary layer and these disturbances was not studied. However, it is the first demonstration of energy-efficient active flow control.

Acknowledgments

The authors thank M. Shepshelovits, Israel Aircraft Industries, for permission to use and modify the airfoil, M. Goldberg for manufacturing the actuators and modifying the airfoil, and T. Bachar, T. Naveh, and E. Nevoh for assistance in developing the actuators and performing the experiments.

References

[1] Seifert, A., Darabi, A., and Wygnanski, I., "On the Delay of Airfoil Stall by Periodic Excitation," *Journal of Aircraft*, Vol. 33, No. 4, 1996, pp. 691–699.

[2] Seifert, A., and Pack, L. G., "Oscillatory Control of Separation at High Reynolds Numbers," AIAA Paper 0214-98, Jan. 1998; also *AIAA Journal* (submitted for publication).

[3] Rae, W. H., Jr., and Pope, A., *Low Speed Wind Tunnel Testing*, 2nd ed., Wiley, New York, 1984, pp. 349–361.

[4] Lin, J. C., Selby, G. V., and Howard, F. G., "Exploratory Study of Vortex-Generating Devices for Turbulent Flow Separation Control," AIAA Paper 91-0042, Jan. 1991.

M. Samimy
Associate Editor

Use of Analytical Flow Sensitivities in Static Aeroelasticity

Richard W. Newsome*
Allison Advanced Development Company, Indianapolis, Indiana 46206
and
Gal Berkooz† and Rajesh Bhaskaran‡
Beam Technologies, Inc., Ithaca, New York 14850

Introduction

MODERN computational fluid dynamics tools can be used to predict sensitivities for flows encountered by aircraft and missiles throughout the flight regime. In this study, we describe one important multidisciplinary application of aerodynamic sensitivity analysis, namely, the coupling of the aerodynamic sensitivities with a structural dynamics analysis and optimization code. Coupling aerodynamic and structural models provides a powerful tool for predicting and controlling both static and dynamic aeroelastic phenomena.

The flow is modeled using the two-dimensional Euler equations. The flow sensitivity is calculated using the sensitivity equation or the analytical sensitivity method. In this approach, equations for the sensitivities are formed by differentiating the flow-governing equations and boundary conditions and then discretizing. References 1 and 2 have previously applied the analytical sensitivity method to the Euler equations. Sensitivity solutions were carried out for two-dimensional subsonic and transonic flow over an airfoil. The sensitivity to change in geometry was incorporated into the ASTROS structural analysis code in place of linear aerodynamic (panel-method-based) sensitivity to calculate static aeroelastic effects in a noniterative fashion. Results are presented for a wing section in transonic flow mounted on a torsion spring for which the geometry variation is due to deformation as well as rotation.

Sensitivity Analysis

The sensitivity equations are obtained by differentiating the Euler equations with respect to the design variables d_k. Details of the

Received Nov. 7, 1996; revision received March 26, 1998; accepted for publication May 4, 1998.

* Systems Manager, F120 Engine Program, P.O. Box 7162, XB12. Associate Fellow AIAA.
† President, 110 N. Cayuga Street.
‡ Staff Scientist, 110 N. Cayuga Street. Member AIAA.